International Journal of Modern Physics C
Vol. 20, No. 9 (2009) 1443–1456
© World Scientific Publishing Company

World Scientific
www.worldscientific.com

Int. J. Mod. Phys. C 2009.20:1443-1456. Downloaded from www.worldscientific.com
by UNIVERSITY OF MICHIGAN on 09/18/15. For personal use only.

MESOSCALE COMPUTER SIMULATIONS OF POLYMER-TETHERED ORGANIC/INORGANIC NANOCUBE SELF-ASSEMBLY

ELAINE R. CHAN* and LIN C. HO*

Department of Chemical Engineering, University of Michigan
2300 Hayward Street, Ann Arbor, MI 48109-2136, USA
** erchan@umich.edu*
† lho@umich.edu

SHARON C. GLOTZER

Departments of Chemical Engineering and Materials Science & Engineering
University of Michigan 2300 Hayward Street, Ann Arbor, MI 48109-2136, USA
sglotzer@umich.edu

A molecular simulation study of the mesoscale self-assembly of tethered nanoparticles having a cubic geometry is presented. Minimal models of the tethered nanocubes are developed to represent a polyhedral oligomeric silsesquioxane (POSS) molecule with polymeric substituents. The models incorporate some of the essential structural features and interaction specificity of POSS molecules, and facilitate access to the long length and timescales pertinent to the assembly process while foregoing atomistic detail. The types of self-assembled nanostructures formed by the tethered nanocubes in solution are explored via Brownian dynamics simulations using these minimal models. The influence of various parameters, including the conditions of the surrounding medium, the molecular weight and chemical composition of the tether functionalities, and the number of tethers on the nanocube, on the formation of specific structures is demonstrated. The role of cubic nanoparticle geometry on self-assembly is also assessed by comparing the types of structures formed by tethered nanocubes and by their flexible coil triblock copolymer and tethered nanosphere counterparts. Morphological phase diagrams are proposed to describe the behavior of the tethered nanocubes.

Keywords: Self-assembly; nanoparticle; simulation; morphology; silsesquioxane.

1. Introduction

Self-assembly is a promising route for generating nanostructured materials with precise properties.[1] Soft materials such as block copolymers and surfactants

*Present address: National Institute of Standards and Technology, Electronics and Electrical Engineering Laboratory, Semiconductor Electronics Division, 100 Bureau Drive, Gaithersburg, MD 20899-8120, USA.

self-assemble into rich morphologies, including lamellar, cylindrical, ordered micellar, and gyroid structures. The type of structure formed depends on the molecular composition, degree of incompatibility between the blocks, and sequence of the blocks in the copolymer. Advances in the syntheses of nanoparticles with macromolecular tethers attached[2] have motivated investigations aimed at elucidating and understanding the self-assembly principles for these nanoscale building blocks (NBBs). A wide variety of NBBs have been synthesized and functionalization of these objects with bio- and synthetic polymers provides new opportunities for creating nanoparticle/polymer assemblies with novel or enhanced properties.

Knowledge of the atomic- and nanoscale processes that occur during the assembly process is important for successful fabrication of materials composed of nanoparticle/polymer assemblies. In conjunction with experiments, molecular simulation is a useful tool for examining self-assembly in nanoscale systems because it affords efficient and systematic exploration of the large parameter space. Specifically, the development and application of multiscale modeling and simulation techniques are necessary to enable bridging of the various length and timescales involved in nanoscale self-assembly. Atomistic simulations are computationally prohibitive because of the large number of molecules that must be employed to probe bulk self-assembly behavior. Furthermore, self-assembled structures that form on longer timescales may not be observed in these simulations, as the inclusion of atomistic detail results in reduced simulation times compared to mesoscale simulations. Thus, it is desirable to develop simpler mesoscale models that enable investigations of self-assembly at long length and timescales.

Presented herein are Brownian dynamics simulation results of tethered nanocube self-assembly. For the present work, the tethered nanocube is regarded as a "minimal" representation of a polyhedral oligomeric silsesquioxane (POSS) cube with polymeric substituents, although its applicability to platinum[3] and gold and silver[4] nanocubes, and general systems of cuboids,[5] with tethers attached at the cube corners may also be considered. Tethered POSS molecules possess a hybrid organic/inorganic character that renders them attractive for constructing nanostructured materials with useful properties.[6] We summarize here our simulation findings on the types of bulk structures that arise from self-assembly of polymer-tethered POSS in solution, and demonstrate how various parameters, including the conditions of the surrounding medium, the molecular weight and chemical composition of the tether functionalities, and the number of tethers on the nanocube, influence the formation of specific structures. Furthermore, we assess the influence of the cubic nanoparticle geometry on the resulting morphologies by comparing self-assembly of tethered nanocubes and of their tethered nanosphere and flexible coil triblock copolymer counterparts. The reader is referred to earlier works for supplementary details.[7–10]

Int. J. Mod. Phys. C 2009.20:1443-1456. Downloaded from www.worldscientific.com
by UNIVERSITY OF MICHIGAN on 09/18/15. For personal use only.

Int. J. Mod. Phys. C 2009.20:1443-1456. Downloaded from www.worldscientific.com
by UNIVERSITY OF MICHIGAN on 09/18/15. For personal use only.

2. Minimal Model Development

Lee and Neurock initially performed *ab initio* DFT calculations on tetrasubstituted POSS $H_4(C_6H_5)_4Si_8O_{12}$ ($cyhex_4$-POSS) to gain insight on the nature of the intermolecular interactions between and structural deformations of the silsesquioxane cages.[7] Such insight provides preliminary guidelines for how to describe the interactions and the cage structure in a mesoscale minimal model. Information on the intermolecular interactions between cage faces without tethers attached and the extent to which these interactions affect cage structure was sought. Three key features established from the *ab initio* calculations that will be used as guidelines in the development of a preliminary minimal model are the following:

(1) there is very little distortion in the structures (i.e. cage bond lengths and bond angles) of interacting functionalized POSS molecules,
(2) the electron density distribution of POSS remains cubic in form for both the "bare" hydrido-functionalized cage and the organic tethered systems, and thus the cubes may be approximated as rigid, and
(3) there is a weak attraction between POSS cubes with a preferred minimum intercube distance.

The pertinent findings from the DFT studies are reported in detail elsewhere.[7] We have developed simplified models of tethered POSS molecules as illustrated in Figs. 1 and 2(a). The cage is modeled as a rigid cube with eight beads comprising the cube vertices and connected by perfectly rigid bonds. Each bead represents groups of atoms on the silsesquioxane cage. For simplicity we assume here that the R substituents on the nontethered silicon corners can be grouped together with atoms that are represented by the vertices of the cube in the minimal model. Each polymer tether on the NBBs is modeled as a chain of soft spheres or monomers that interact via a bond stretching potential. Pairs of successive monomers along

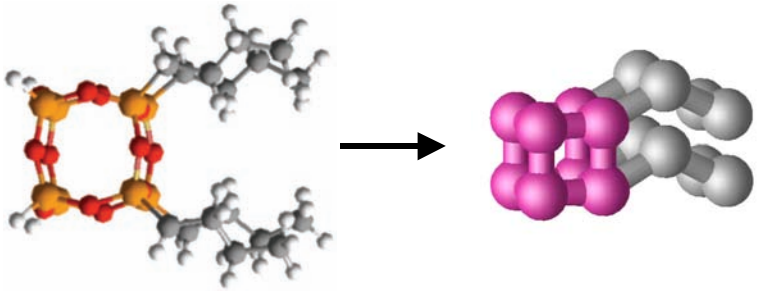

Fig. 1. Representation of a tetratethered POSS molecule $R'_4R_4Si_8O_{12}$ (left) by the minimal model (right). There are four homopolymer tethers R′ each attached to silicon atoms that comprise the same face of the cubic cage. In the atomistic representation, the silicon atoms are denoted in orange, carbon atoms in grey, oxygen atoms in red, and hydrogen atoms in white.

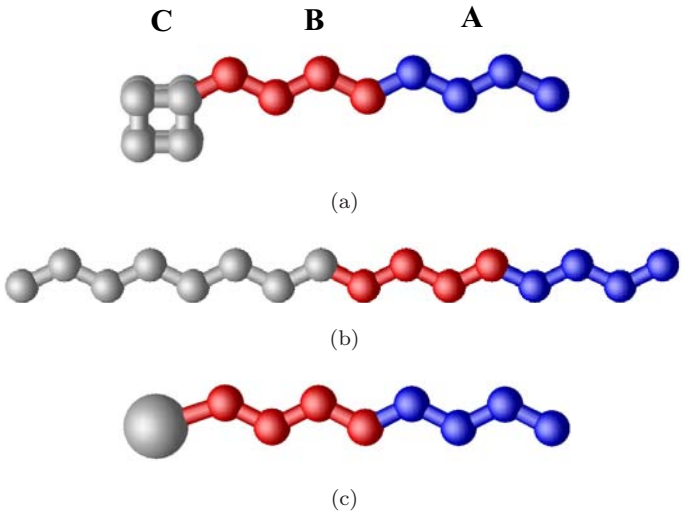

Fig. 2. Representations of model monotethered NBBs with a diblock copolymer tether attached to either a nanoparticle or its linear chain counterpart. (a) ABC diblock copolymer tethered nanocube. (b) Linear ABC triblock copolymer. (c) ABC diblock copolymer tethered nanosphere.

Int. J. Mod. Phys. C 2009.20:1443-1456. Downloaded from www.worldscientific.com
by UNIVERSITY OF MICHIGAN on 09/18/15. For personal use only.

a chain interact via a finitely extensible nonlinear elastic (FENE)[11] anharmonic spring potential.

To simulate phase separation arising from selectivity of the implicit solvent for cube beads or tether monomers, the interactions in the model are denoted as the following.[12] If the solvent is poor for one particle species, then that species will interact via an attractive potential. Conversely, if the solvent is good for a particular species, then that species will interact via a purely repulsive potential. As the cube beads and tether monomers are considered different species, they also interact via this purely excluded volume interaction to mimic immiscibility between them. Attractive interactions between beads are captured using a truncated and shifted Lennard–Jones (LJ) 12-6 potential,[13,14] which accounts for both excluded volume and van der Waals interactions. The site-site interactions between cube beads and tether monomers are captured by a purely repulsive Weeks–Chandler–Andersen[15] (WCA) soft-sphere potential. This potential is intended to mimic immiscibility between different bead species.

3. Simulation Methodology

Brownian dynamics is a stochastic molecular dynamics simulation method used to simulate self-assembly of the tethered nanocubes and linear block copolymers in implicit solvent. The equation of motion for each bead i is

$$m_i \dot{\mathbf{v}}_i(t) = -m_i \xi_i \mathbf{v}_i(t) + \mathbf{F}_i(\mathbf{x}_i(t)) + \mathbf{R}_i(t)\,, \tag{1}$$

where m_i is the mass of bead i, and $\mathbf{x}_i$, $\mathbf{v}_i$, $\mathbf{F}_i$, and ξ_i represent the position, velocity, force, and friction coefficient acting on bead i, respectively.[16] These simulations

Int. J. Mod. Phys. C 2009.20:1443-1456. Downloaded from www.worldscientific.com
by UNIVERSITY OF MICHIGAN on 09/18/15. For personal use only.

sample the canonical ensemble because the friction coefficient and stochastic noise term couple the system to a heat bath and thereby function together as a nonmomentum conserving thermostat.

Reduced units are used in which the basic units for length and energy are σ and ε of the LJ potential, respectively. Each cube bead and tether monomer has the same size $\sigma = 1$ and mass $m = 1$. The simulation results are presented in terms of these reduced units; thus, the reduced temperature is defined as $T^* = k_BT/\varepsilon$, the interaction energy parameter as $\varepsilon^* = \varepsilon/k_BT$, the reduced timestep as $\Delta t = t/\sigma\sqrt{m/\varepsilon}$, and the reduced friction coefficient as $\xi^* = \xi\sigma\sqrt{m/\varepsilon}$. Boltzmann's constant is denoted as k_B. The concentration of molecules in the system is based on the reduced number density of particles $\rho^* = N\sigma^3/V$, where N denotes the sum of cube beads and tether monomers and V is the volume of the simulation box.

The simulations are performed using cubic simulation boxes and periodic boundary conditions. The equations of motion are integrated using the leap-frog algorithm[14] with timestep $\Delta t = 0.01$. ξ^* is set to unity for each particle so that the simulations are performed in the range between overdamped and purely deterministic regimes.[17] The method of quaternions[14] is utilized to simulate rigid-body motion of the cube. Each system is first relaxed athermally (i.e. only excluded volume interactions, $\varepsilon^* = 0$) to generate an initial disordered configuration. The systems are subsequently cooled in small increments to map out morphological phase diagrams and help prevent the systems from getting trapped into metastable states. Because nonequilibrium structures can depend on the cooling history, both the size of the temperature increments at which the initial athermal configurations are cooled to the target temperature, as well as the system size Nb, are varied to verify that the same equilibrium structures form. The structural evolution of each system is monitored as a function of time by inspecting snapshots of configurations.

4. Tetratethered Nanocube Self-Assembly Studies

Self-assembly of tetratethered nanocubes are investigated under the good solvent condition for the tether monomers and poor solvent condition for the cube beads, i.e. cube-cube (CC) interactions are of the LJ type and tether-tether (TT) and cube-tether (CT) interactions are both of the WCA type. The simulated systems contain $Nb = 400$ and 1000 NBBs having homopolymer tethers, and each tether consists of $Nt = 2$ monomers ($N = 6400$ and 16 000, respectively) or $Nt = 4$ monomers ($N = 9600$ and 24 000, respectively). We summarize our findings pertaining to self-assembly here and refer the reader to an earlier publication for further details and discussion.[7]

Figure 3 displays snapshots of equilibrium configurations of $Nb = 400$ tethered nanocubes with short tether lengths $Nt = 2$ at concentrations $\rho^* = 0.76$, 0.67, and 0.57 and $\varepsilon^* = 0.8$. These values of concentration represent a progression from melt-like systems to systems in solution that is good for the tethers and poor for the cubes. Assembly of the NBBs into hexagonally arranged cylindrical phases of cubic

Int. J. Mod. Phys. C 2009.20:1443-1456. Downloaded from www.worldscientific.com
by UNIVERSITY OF MICHIGAN on 09/18/15. For personal use only.

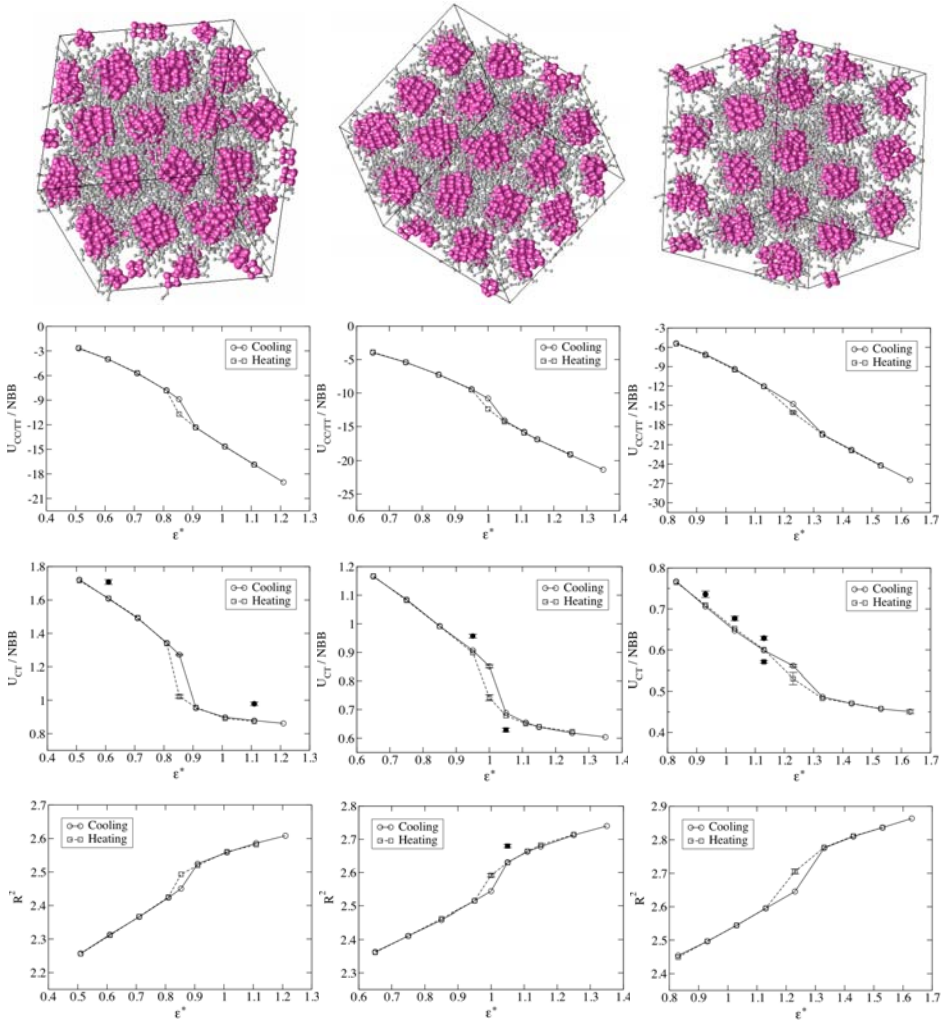

Fig. 3. Final equilibrium configurations obtained via cooling, and the variation of the nonbonded pair interaction energies and average tether mean squared corner-to-end distance with ε^*, for (a) $\rho^* = 0.76$, (b) $\rho^* = 0.67$, and (c) $\rho^* = 0.57$. Error bars are shown when larger than the symbol. Some error bars are illustrated using filled circles and squares above or below the corresponding open symbols for clarity. The tether monomers ($Nt = 2$) are reduced in size in the simulation snapshots for clarity.

cross-section, with the cubes comprising the core and the tethers pointing outward, is observed. The simulations required approximately 250 CPU hours on a single Athlon AMD 2400 processor for the structures to form. The square cross-section of each cylinder can be attributed to the cubic geometry of the nanoparticle, and the simulations thereby demonstrate how the shape of the final assembled structures can

Int. J. Mod. Phys. C 2009.20:1443-1456. Downloaded from www.worldscientific.com
by UNIVERSITY OF MICHIGAN on 09/18/15. For personal use only.

be adjusted from round to cubic by merely attaching NBBs of a specific geometry to polymer chains. Further inspection of simulation snapshots reveals a face-to-face local packing of the NBBs within each cylinder. Hence, the minimal model captures features of local packing observed in POSS systems.[18]

The interaction energies between the same species (CC and TT) $U_{\mathrm{CC/TT}}$ and different species (CT) U_{CT} of beads, and average tether mean squared corner-to-end distances R^2, are monitored over a range of ε^* values to estimate order-disorder transitions and phase boundaries (Fig. 3).[19,20] The plots exhibit discontinuous changes upon cooling that signify ordering of the molecules into cylindrical structures with cube-rich and tether-rich regions. Hystereses are observed upon reheating of the systems and suggest that the transition from a disordered state to hexagonally packed cylinders of tethered cubes appears to be first-order as in traditional block copolymer and surfactant systems.

For systems at low concentration in solvent that is selectively good for the tethers and poor for the cubes, the simulations predict that the tethered NBBs self-assemble into micellar phases instead of cylindrical phases. Sufficiently large systems of $Nb = 1000$ NBBs ($N = 16\,000$) are studied to ensure that three-dimensional periodicity present in the equilibrium morphologies are captured. Snapshots of configurations reveal that the micelles consist of the cubes assembled in the core and the tethers pointing outward in accordance with the selective solvent condition. Disordered mixtures of spherical and cylindrical micelles are present, with spherical micelles predominant at dilute concentrations. The principal radii of gyration indicate that micelles containing up to approximately 11 NBBs have a roughly spherical geometry, while larger micelles grow in one direction to form elongated or cylindrical structures. It appears that the cubic shape of the NBB facilitates the formation of the cylindrical micelles, and the tethered nanocubes preferring to pack in a face-to-face manner within these structures.

To investigate the effect of tether length on the self-assembly behavior of the cubic NBBs, simulations of tethered nanocubes with longer tethers each consisting of $Nt = 4$ monomers are performed. The tethered NBBs self-assemble into hexagonally arranged cylinders at high concentrations that correspond closely to the melt state. At lower concentrations the NBBs prefer to self-assemble into micelles that are ordered in a face-centered cubic (FCC)-like packing. The values of the asphericity parameter are less than the maximum value of 0.1 that characterizes spherical objects[21] over the range of aggregate sizes for which the statistics are good. Thus, the longer solvophilic tethers on the NBB induce more curvature in the self-assembled structures and lead to micelles that are essentially spherical in shape. The assembly of the NBBs into a FCC pattern contrasts with the typical self-assembly of diblock copolymers and surfactants into body-centered cubic ordered patterns at low concentrations. The FCC packing observed here may arise from the cubic shape of the nanoparticle.

Morphological phase diagrams for the tethered nanocubes are presented in Fig. 4. Similarities and differences exist between the phase behavior predicted

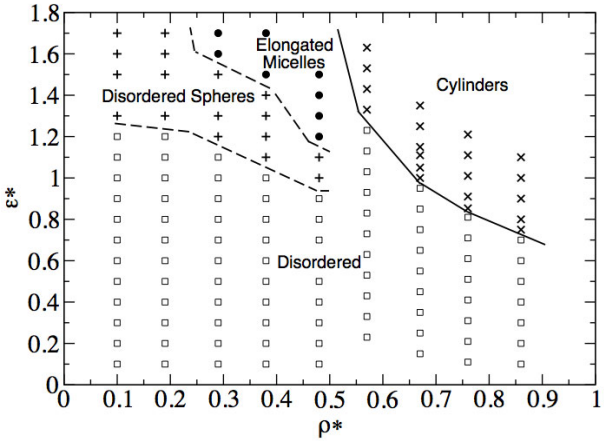

(a)

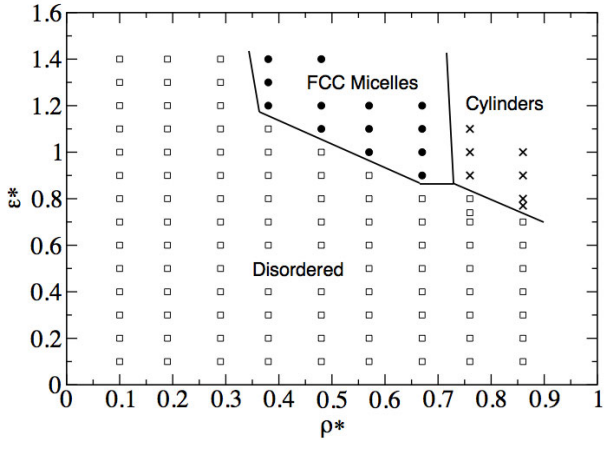

(b)

Fig. 4. Proposed phase diagrams for systems of tetratethered nanocubes. Symbols correspond to simulated state points and the different morphologies observed. Phase boundaries are drawn as guides to the eye. (a) $Nt = 2$. (b) $Nt = 4$.

by simulation for systems of tetratethered nanocubes vs flexible coil surfactants in solution. Nanocubes with short tethers self-assemble into disordered spherical and elongated micelles and hexagonally packed cylinders that resemble the structures observed in flexible coil surfactant systems[19] at similar concentration values. However, assembly of the tethered NBBs at very high concentrations into lamellar phases, which typically evolve in systems of compositionally symmetric surfactants and diblock copolymers, was anticipated and not observed. This phase is absent in the tetratethered nanocube systems because of the unique architecture of this building block. The polymer chains on a single tetratethered NBB exclude a large amount

Int. J. Mod. Phys. C 2009.20:1443-1456. Downloaded from www.worldscientific.com
by UNIVERSITY OF MICHIGAN on 09/18/15. For personal use only.

of free volume that inhibits self-assembly of the cubes into sheet structures. Simulations of monotethered nanocube self-assembly, where the NBBs consist of only one homopolymer tether, reveal that these NBBs have a propensity to self-assemble into structures consisting of alternating sheets of cubes and tethers.[8,10] The lamellae appear to be stabilized by the local face-to-face packing of cubes resulting from the attractive site-site interactions between cubes in the minimal model.

5. Block Copolymer Tethered NBB Self-Assembly Studies

We extend our self-assembly studies of homopolymer tethered nanocubes by examining the types of self-assembled structures arising in systems of diblock copolymer tethered nanocubes (ABC tethered NBBs) under various solvent conditions. Comparisons are made between the structures formed by the ABC tethered nanocubes and those formed by their flexible coil ABC triblock copolymer and ABC tethered nanosphere counterparts (Fig. 2) to gain insight on the influence of cubic nanoparticle shape on self-assembly. We construct minimal models of these molecules as described above and focus on systems of tethered NBBs and block copolymers where the interactions between different blocks or bead types are symmetric. Further details may be found in an earlier work.[8]

Systems of $Nb = 1000$ monotethered NBBs or triblock copolymer chains are simulated using cubic simulation boxes and periodic boundary conditions at $\rho^* = 0.86$ and $T^* = 1$. Each nanosphere has size 2σ and mass 8 m to match the dimensions of a single nanocube. The system concentration is based on the reduced number density of beads $\rho^* = \Sigma_i m_i N_i \sigma_i^3 / V$, where N_i denotes the number of particles of type i (tether bead, cube corner bead, or nanosphere) and V is the volume of the simulation cell.

5.1. *Selective good solvent for the C block*

Under conditions where the solvent is selectively good for the C block (i.e. cubes and linear C blocks are solvophilic) and poor for the tethers (i.e. tethers are solvophobic), the interactions between cube beads or linear C block monomers are of the WCA type and the interactions between A tether beads (A-A) and between B tether beads (B-B) are each of the LJ type. The interactions between cube beads are modeled as purely excluded volume to assess the effect of simply attaching the rigid cubic nanoparticle to the copolymer on morphological behavior.

The simulations indicate that the presence of the rigid cube appears to preclude assembly of the NBBs into spherical micelles and influences assembly into lamellar and hexagonally arranged cylindrical phases at relative copolymer tether block fractions that are significantly different from the block fractions that give rise to such structures in linear diblock copolymer systems. Representative simulation snapshots of these structures are presented in Fig. 5.

Replacing the cube by its linear counterpart results in a conventional ABC triblock copolymer where the C end block is comprised of eight beads. Our simulations

Int. J. Mod. Phys. C 2009.20:1443-1456. Downloaded from www.worldscientific.com
by UNIVERSITY OF MICHIGAN on 09/18/15. For personal use only.

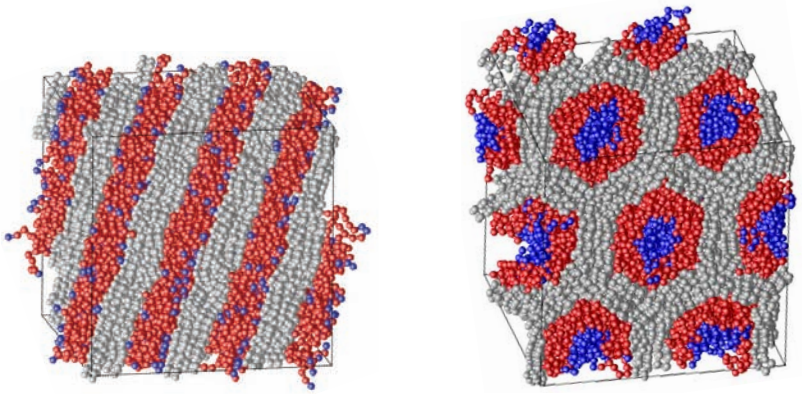

(a) (b)

Fig. 5. (Color online) Simulation snapshots of tethered nanocube equilibrium morphologies in selectively good solvent for the cube. (a) Lamellae at $f_B = 0.875$. (b) Hexagonally arranged core-shell cylinders at $f_B = 0.75$. The A block (blue) comprises the core, the B block (red) the shell, and the C block nanocubes (grey) the matrix.

Int. J. Mod. Phys. C 2009.20:1443-1456. Downloaded from www.worldscientific.com
by UNIVERSITY OF MICHIGAN on 09/18/15. For personal use only.

of the copolymer chains predict self-assembly into lamellar, core-shell cylindrical, and perforated lamellar phases. The latter phase consists of layers composed of A and B tether beads that are punctured by the C end blocks, thereby forming holes in the lamellae. The curved morphologies may arise from the constraint that the linear C end block is compositionally equivalent to the cube (i.e. same value of the relative C block volume fraction f_C), which does not necessarily translate to geometric equivalence between the linear segment and the cube. The lamellar and perforated lamellar structures may occur because of the short tether lengths studied here to satisfy the constraint that both the C block segment and the nanocube have equal composition.

To further investigate the effect of geometry on self-assembly between the linear triblock copolymer and tethered nanocube systems, simulations of "modified," or geometrically equivalent, triblock chains are also performed. Our simulations suggest that modified triblock copolymers exhibit a propensity to self-assemble into lamellae. Compared to the tethered nanocube systems, the modified triblock chains do not form curved cylindrical morphologies. Thus, the presence of the rigid cubic nanoparticle appears to induce curvature in the tethered nanocube morphologies.

5.2. *Neutral poor solvent for all blocks*

Under conditions where the solvent is neutrally poor for each bead species, the interactions between the same species of beads (A-A, B-B, C-C) are each of the LJ type. Our simulations predict that both ABC tethered nanocubes and their linear triblock copolymer counterparts self-assemble into solely lamellar structures under this solvent condition. The sheets exhibit an ABCCBA sequence because of the

attractive interactions in the model between the same species of beads. However, a fundamental difference exists in the local intermolecular packing of the C-rich layers in both systems. The cubes are packed in a distinct face-to-face arrangement, while the C-rich layers exhibit no clear ordering of monomers within them in the linear triblock copolymer systems. The absence of cylindrical phases in the neutral poor solvent conditions suggests that the local face-to-face intermolecular packing of the cubes strongly stabilizes lamellar structures, as was demonstrated in a recent simulation study of homopolymer tethered nanocube self-assembly.[10]

5.3. *Selective poor solvent for the C block*

Lastly, self-assembly is examined under the condition where the solvent is selectively poor for the C block (cubes and linear C end block) and good for the tethers. The interactions between C block beads are of the LJ type and the A-A and B-B tether bead interactions are each of the WCA type. The simulations predict self-assembly of the tethered nanocubes and linear triblock copolymers into exclusively lamellar morphologies under this solvent condition. These findings are similar to the neutral poor solvent results. However, inspection of simulation snapshots reveals that the lamellae in these systems do not exhibit the ABCCBA sequence of sheets. In the case of the tethered nanocubes, the tether beads form layers in which the A blocks and B blocks are mixed, while the cubes remain organized in a well-defined face-to-face pattern within cube-rich layers. The flexible coil triblock copolymers also display mixing of the tether A and B blocks within tether-rich layers and there is no ordering present within the C-rich layers. The mixing within the tether bead layers occurs as a consequence of the nature of the repulsive interactions between the tether beads.

5.4. *Comparisons between ABC tethered nanosphere and ABC tethered nanocube self-assembly*

It is interesting to examine how the geometry of a cubic nanoparticle affects self-assembly compared to a spherical nanoparticle shape. For the case where the solvent is selectively good for the nanoparticle and poor for the tether, simulations of diblock copolymer tethered nanosphere self-assembly with $f_B = 0.75$ predict formation of core-shell cylinders arranged in a hexagonal pattern [Fig. 6(a)]. This phase is also observed in simulations of the compositionally equivalent tethered nanocubes and linear triblock copolymer chains, but the cylindrical structures in the tethered nanosphere systems have a round cross-section, while those formed by the tethered nanocubes have a distinct hexagonal cross-section [Fig. 5(b)]. The hexagonal shaped cylinders have flat edges that are promoted by the flat faces of the rigid cubes. Further conclusion can be made that the rigidity of the cubic or spherical nanoparticle induces curvature in the assembled structures, because the cylindrical morphology differs from the lamellar structures observed in the simulations of the modified (geometrically equivalent) linear triblock copolymers.

Int. J. Mod. Phys. C 2009.20:1443-1456. Downloaded from www.worldscientific.com
by UNIVERSITY OF MICHIGAN on 09/18/15. For personal use only.

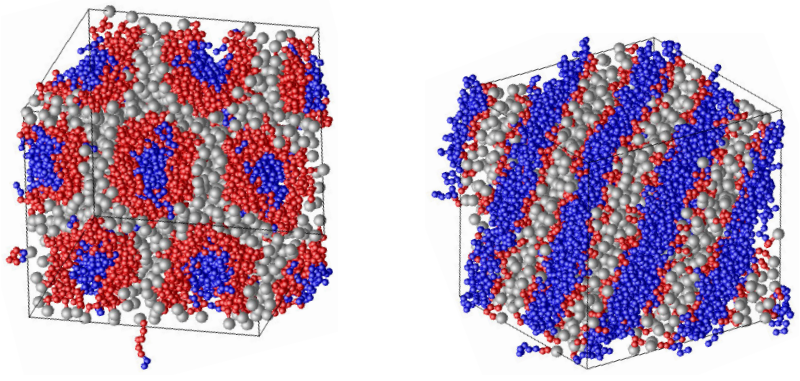

(a) (b)

Fig. 6. Simulation snapshots of diblock copolymer tethered nanosphere morphologies. (a) Core-shell cylinders are observed in selective good solvent at $f_B = 0.75$. (b) Lamellae in an ABCCBA pattern are observed in neutral poor solvent at $f_B = 0.25$.

To investigate the effect of changing the composition of the polymer tether on phase behavior of the tethered NBBs, the simulated structures of the diblock copolymer tethered nanosphere are compared with those predicted for the corresponding homopolymer functionalized nanospheres from simulation.[22] The simulations predict that the diblock copolymer tethered nanospheres assemble into core-shell cylindrical structures while the homopolymer tethered nanospheres assemble into lamellar sheets. Hence, the composition of the polymer tether can influence the type of morphology formed in the tethered nanosphere systems.

Additional tethered nanosphere systems of varying f_B and solvent quality are examined. In neutral poor solvent, lamellar phases arise for low and intermediate relative B block fractions and the sheets exhibit an ABCCBA pattern [Fig. 6(b)]. Although the tethered nanocubes also display this precise morphology at the corresponding f_B values, the ordering of NBBs within the C-rich sheets [Fig. 5(a)] is absent in the corresponding tethered nanosphere structures. At high f_B values the simulations predict core-shell cylinder morphologies, in contrast with the lamellae observed in the tethered nanocube systems. This result further supports the notion that the face-to-face local packing of the cubes stabilizes lamellar structures.

6. Conclusions

Simplified mesoscale models of tethered nanocubes representing POSS molecules with polymeric functional groups have been developed and utilized in Brownian dynamics simulations to investigate self-assembly of the NBBs. The influence of solvent quality, temperature, NBB concentration, tether chemical composition, and tether number on the resulting assemblies was examined. It was demonstrated that tethered nanocubes self-assemble into structures that are analogous to those observed in block copolymer and surfactant systems. Morphological phase diagrams

Int. J. Mod. Phys. C 2009.20:1443-1456. Downloaded from www.worldscientific.com
by UNIVERSITY OF MICHIGAN on 09/18/15. For personal use only.

for tetratethered nanocubes were constructed and found to share qualitative similarities with the phase diagrams for surfactant solutions, as well as differences that were attributed to the unique geometry and architecture of the tethered NBB. Simulations of ABC block copolymer tethered nanocubes, flexible coil ABC triblock copolymers, and ABC monotethered nanospheres were also conducted to gain insight on the influence of nanocube geometry on self-assembly. These simulations suggested that cubic nanoparticle geometry plays a significant role in inducing curvature in the self-assembled morphologies under certain solvent conditions. Additional efforts to improve the accuracy of the minimal models via coarse-graining schemes have been undertaken to rigorously investigate tethered nanocube self-assembly in solution.[23]

Int. J. Mod. Phys. C 2009.20:1443-1456. Downloaded from www.worldscientific.com
by UNIVERSITY OF MICHIGAN on 09/18/15. For personal use only.

Acknowledgments

Funding for this work was provided by the National Science Foundation under Grant No. DMR-0103399. We are grateful to P. T. Cummings, J. Kieffer, C. McCabe, M. Neurock, C.-Y. Lee and A. Striolo for insightful discussions and collaboration on modeling POSS/polymer assemblies. The University of Michigan Center for Advanced Computing is acknowledged for computer cluster support.

References

1. S. C. Glotzer, M. J. Solomon and N. A. Kotov, *AIChE J.* **50**, 2978 (2004).
2. A. K. Boal, F. Ilhan, J. E. DeRouchey, T. Thurn-Albrecht, T. P. Russell and V. M. Rotello, *Nature* **404**, 746 (2000); W. J. Parak, T. Pellegrino, C. M. Micheel, D. Gerion, S. C. Williams and A. P. Alivisatos, *Nano Lett.* **3**, 33 (2003); G. Cardoen and E. B. Coughlin, *Macromolecules* **37**, 5123 (2004); C.-C. Chu, T.-I. Ho and L. Wang, *Macromolecules* **39**, 5657 (2006).
3. T. S. Ahmadi, Z. L. Wang, T. C. Green, A. Henglein and M. A. El-Sayed, *Science* **272**, 1924 (1996).
4. Y. G. Sun and Y. N. Xia, *Science* **298**, 2176 (2002).
5. B. S. John, A. Stroock and F. A. Escobedo, *J. Chem. Phys.* **120**, 9383 (2004).
6. R. Knischka, F. Dietsche, R. Hanselmann, H. Frey, R. Mulhaupt and P. J. Lutz, *Langmuir* **15**, 4752 (1999); B. S. Kim and P. T. Mather, *Macromolecules* **35**, 8378 (2002); K. M. Kim, D. K. Keum and Y. Chujo, *Macromolecules* **36**, 867 (2003); R. M. Laine, *J. Mater. Chem.* **15**, 3725 (2005).
7. E. R. Chan, X. Zhang, C.-Y. Lee, M. Neurock and S. C. Glotzer, *Macromolecules* **38**, 6168 (2005).
8. E. R. Chan, L. C. Ho and S. C. Glotzer, *J. Chem. Phys.* **125**, 064905 (2006).
9. S. C. Glotzer, M. A. Horsch, C. R. Iacovella, Z. L. Zhang, E. R. Chan and X. Zhang, *Curr. Opin. Colloid Interface Sci.* **10**, 287 (2005).
10. X. Zhang, E. R. Chan and S. C. Glotzer, *J. Chem. Phys.* **123**, 184718 (2005).
11. G. S. Grest and K. Kremer, *Phys. Rev. A* **33**, 3628 (1986).
12. Z. L. Zhang, M. A. Horsch, M. H. Lamm and S. C. Glotzer, *Nano Lett.* **3**, 1341 (2003).
13. A. R. Leach, *Molecular Modeling: Principles and Applications*, 2nd edn. (Prentice Hall, Harlow, 2001).
14. M. P. Allen and D. J. Tildesley, *Computer Simulation of Liquids* (Clarendon Press, Oxford, 1987).

15. J. D. Weeks, D. Chandler and H. C. Andersen, *J. Chem. Phys.* **54**, 5237 (1971).
16. W. F. van Gunsteren, H. J. C. Berendsen and J. A. C. Rullmann, *Mol. Phys.* **44**, 69 (1981); G. S. Grest, M. D. Lacasse, K. Kremer and A. M. Gupta, *J. Chem. Phys.* **105**, 10583 (1996).
17. K. H. Kim, S. H. Kim, J. Huh and W. H. Jo, *J. Chem. Phys.* **119**, 5705 (2003).
18. G. Calzaferri, R. Imhof and K. W. Tornroos, *J. Chem. Soc., Dalton Trans.*, 3123 (1994); T. P. E. Auf der Heyde, H. B. Burgi, H. Burgy and K. W. Tornroos, *Chimia* **45**, 38 (1991).
19. R. G. Larson, *J. Chem. Phys.* **96**, 7904 (1992).
20. H. Guo and K. Kremer, *J. Chem. Phys.* **119**, 9308 (2003).
21. M. Kenward and M. D. Whitmore, *J. Chem. Phys.* **116**, 3455 (2002).
22. C. R. Iacovella, M. A. Horsch, Z. L. Zhang and S. C. Glotzer, *Langmuir* **21**, 9488 (2005).
23. E. R. Chan, A. Striolo, C. McCabe, P. T. Cummings and S. C. Glotzer, *J. Chem. Phys.* **127**, 114102 (2007).

Int. J. Mod. Phys. C 2009.20:1443-1456. Downloaded from www.worldscientific.com
by UNIVERSITY OF MICHIGAN on 09/18/15. For personal use only.